



Published in final edited form as:

*Regen Eng Transl Med.* 2023 September ; 9(3): 424–430. doi:10.1007/s40883-022-00292-9.

## Injectable neural hydrogel as *in vivo* therapeutic delivery vehicle

Nora Hlavac<sup>1</sup>, Deanna Bousalis<sup>1</sup>, Emily Pallack<sup>1</sup>, Yuan Li<sup>1</sup>, Eleana Manousiouthakis<sup>1</sup>, Raffae Ahmad<sup>1</sup>, Christine E. Schmidt<sup>1</sup>

<sup>1</sup>Biomedical Engineering, University of Florida, Gainesville, FL, US

### Abstract

**Purpose**—This study demonstrated *in vivo* delivery of a decellularized, injectable peripheral nerve (iPN) hydrogel and explored options for using iPN in combination with regenerative biomolecular therapies like stem cell secretome.

**Methods**—Rat-derived iPN hydrogel solutions were combined with a dextran-dye before subcutaneous injection into adult Sprague Dawley rats. After injection, an *in vivo* imaging system (IVIS) was used to visualize hydrogels and quantify dextran-dye release over time. Poly(lactic-co-glycolic) acid (PLGA) was used to encapsulate the dextran-dye to prolong molecular release from the hydrogel scaffolds. Lastly, we investigated use of adipose-derived stem cell (ASC) secretome as a potential future combination strategy with iPN. ASC secretome was assessed for growth factor levels in response to media stimulation and was encapsulated in PLGA to determine loading efficiency.

**Results**—Gelation of iPN hydrogels was successful upon subcutaneous injection. When combined with iPN, a 10 kDa dextran-dye was reduced to 54% its initial signal at 24 hours, while PLGA-encapsulated dextran-dye in iPN was only reduced to 78% by 24 hours. Modified media stimulation resulted in changes in ASC phenotype and dramatic upregulation of VEGF secretion. The PLGA encapsulation protocol was adapted for use with temperature sensitive biomolecules, however, considerations must be made with loading efficiency for cell secretome as the maximum efficiency was 28%.

**Conclusion**—The results of this study demonstrated successful injection and subsequent gelation of our iPN hydrogel formulation *in vivo*. Biomolecular payloads can be encapsulated in PLGA to help prolong their release from the soft iPN hydrogels in future combination therapies.

**Lay Summary**—We developed an injectable decellularized tissue scaffold from rat peripheral nerve tissue (called iPN), a potential minimally invasive therapeutic meant to fill lesion spaces after injury. This study was the first demonstration of iPN delivery to a living animal. The iPN solution was injected subcutaneously in a rat and properly formed a gelled material upon entering the body. Our results showed that encapsulating biomolecules in an FDA-approved polymer (PLGA) slowed the release of biomolecules from the iPN, which could allow therapeutics more

---

Corresponding Author: Christine E. Schmidt, schmidt@bme.ufl.edu.

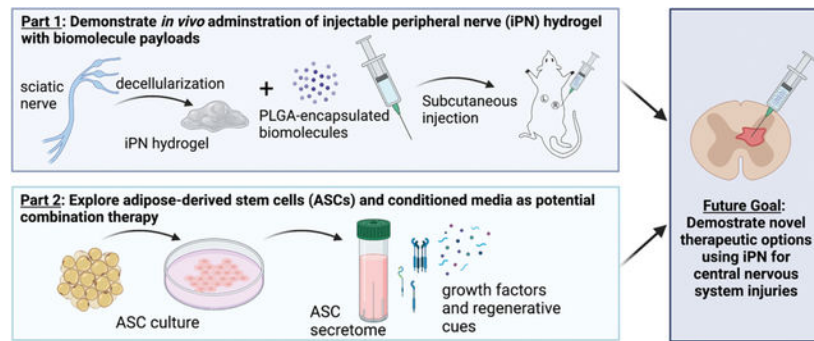
Statements and Declarations

The authors have no financial interests to disclose. All authors contributed to study design, material preparation and/or experiments. Nora Hlavac completed experimental analyses and wrote the first draft of the manuscript. All authors read and approved the manuscript.

time around the scaffold to help repair native tissue. Lastly, we investigated one potential avenue for combining iPN with other regenerative cues obtained from adipose-derived stem cells.

**Description of Future Works**—Future work must focus on optimal loading conditions and release profiles from the iPN hydrogels. Next steps will be applying iPN in various combination therapies for spinal cord injury. We will focus efforts on developing a pro-regenerative secretome that directly promotes neurite extension and neural cell infiltration into iPN scaffolds upon transplantation in spinal cord.

## Graphical Abstract



## Keywords

Hydrogel; injectable; PLGA; ASCs; secretome; decellularized tissue; spinal cord injury

## Introduction

Central nervous system (CNS) injuries comprise a large portion of life-altering, chronic conditions in patients, with millions of brain and spinal cord injuries occurring every year in the United States [1]. Combination therapies involving cellular, molecular, and biomaterial components are the current goal for researchers addressing the complexities of CNS injury [2–4]. Specifically, hydrogels have become an attractive option as soft tissue-mimicking scaffolds that can be easily combined with cell transplants or therapeutics. Further, injectable hydrogels are ideal for filling irregularly shaped brain or spinal cord lesions.

We previously developed and characterized an injectable hydrogel derived from decellularized native peripheral nerve tissue (“iPN hydrogel”) [5,6]. iPN contains necessary components for neural cell survival and reparative extracellular matrix proteins like laminin and various collagen. It also has been mechanically matched to soft CNS tissue [5,6] and is a therapeutically relevant harvest option. Results of our studies showed potential for the iPN hydrogels to be used in combination therapies with transplantable cells and biomolecules. In Bousalis et al., we demonstrated that PLGA encapsulation of biomolecules was essential to achieve payload delivery from iPN hydrogels over days rather than hours [6]. However, to date, we have not demonstrated iPN hydrogel delivery *in vivo*.

While our studies show that iPN hydrogels support neural cell viability [6,7], we are also interested in cell-free therapeutics that may augment the regenerative capability of iPN upon delivery to CNS lesions without the complications of cell transplantation. Cell-free therapies include biomolecular cues that may be in the form of cell “secretome” [8]. Adipose-derived stem cells (ASCs) are an attractive option for generating secretome as they secrete both neural-specific and wound healing growth factors, are abundant, and can be procured through liposuction [9,10]. Previous studies found that ASCs and their secretome promote neurite outgrowth and gene fold expression of neural and wound healing growth factors in a model system [11,12]. Moreover, ASCs can be primed towards a neural-like phenotype by specified molecular cues in the media, such as retinoic acid, B27, and fibroblast growth factor-basic (b-FGF) [13]. We investigated whether similar modified media conditions may prime ASCs to secrete higher levels of regenerative growth factors as well.

This study (1) demonstrates that iPN hydrogels are injectable and appropriately gel *in vivo*, (2) investigates the use of PLGA encapsulation for biomolecular release from iPN hydrogels *in vivo*, and (3) introduces a potential combination therapy for CNS injuries involving stem cell secretome. Moreover, we assessed release profiles for free and encapsulated biomolecules from the hydrogels *in vivo*. Lastly, a modified media regime primed ASCs to produce growth factors that may augment regeneration around an iPN scaffold. In the future, we plan to combine the therapeutic modalities of iPN and ASC-derived secretome for delivery to spinal cord injury lesions.

## Methods

### iPN hydrogel preparation

The iPN hydrogels were prepared as described previously [5,6]. Briefly, sciatic nerve tissue was harvested from adult male and female Sprague Dawley rats. All procedures involving animal handling and tissue collection were conducted in accordance with an approved IACUC protocol at the University of Florida. Chemical decellularization [5] using sodium deoxycholate was utilized to efficiently remove cellular content from whole sciatic nerves. Following decellularization, nerves were lyophilized and stored in sterile containers at  $-20^{\circ}\text{C}$  until solubilization for hydrogel solution preparation.

### Poly(lactic-co-glycolic acid) (PLGA) encapsulation

PLGA was used to encapsulate either a model payload (dye-tagged dextran) for *in vivo* investigations or cell secretome for loading concentration studies. Protocols were identical to those described in Bousalis et al. [6], except for incubations being performed on ice (instead of room temperature) when preparing samples with cell secretome, to account for temperature-sensitive growth factors that may be used in combination therapies. Particle size was verified by imaging on a Leica DM IL LED inverted microscope. Particles were lyophilized prior to storage at  $-20^{\circ}\text{C}$ . For cell secretome, 1 mL of concentrated media was used per 10 mL of 5% (w/v) PLGA in dichloromethane, and for dye-tagged dextran, 2 mg dye was combined with 5 mL of 5% (w/v) PLGA in dichloromethane.

## Subcutaneous injections and IVIS imaging

A 10 kDa dextran-Alexa Fluor 680 dye (Fisher Scientific D34680, referred to henceforth as dye) was integrated into the iPN to visualize the injection and investigate diffusivity from the iPN scaffold (since 10kDa is of similar size to growth factors of interest for combination therapeutics). Prior to injection, male Sprague Dawley rats (250–300g) were anesthetized using isoflurane. Two study conditions were prepared (n=3/condition): (1) PLGA-encapsulated dye in hydrogel (3.75 mg particles/150  $\mu$ L hydrogel) and (2) dye in hydrogel (100 picomoles dye/150  $\mu$ L hydrogel). For baseline comparison, one rat was injected with PLGA-encapsulated dye (3.75 mg particles/150  $\mu$ L saline) and free dye (100 picomoles/150  $\mu$ L saline) without hydrogel. Injection volumes were 100  $\mu$ L of designated solution.

Each rat received two injections in the mid-region of their back (on either side of the midline) and were immediately placed into a Perkin Elmer IVIS Spectrum (*in vivo* Imaging System) for imaging. Animals were imaged 10 times every three minutes, beginning immediately after injection, and then were imaged at 6, 12, 24, 48, and 72 hours post injection. Release kinetics were assessed at the injection site by quantifying the normalized average radiant efficiency in a selected region of interest (ROI), as indicated in Figure 1a. Each ROI was normalized to a value of 1.0 at 0 hours.

## ASC culture conditions

Human ASCs (Lonza PT-5006) from three individual donors, referred to herein as ASC batches, were cultured in growth medium made of DMEM/F12 (Caisson Labs DFL15) and 10% fetal bovine serum (Atlanta Biologicals S11150). Passage 1–4 ASCs were seeded into six-well plates for experimentation ( $1 \times 10^5$  cells/well). After seeding, cells were grown for 24 hours, then the medium was switched to the secretion medium for 72 hours. Two secretion media were assessed: (1) plain neurobasal medium (Thermo Fisher 12348017) and (2) modified medium (similar to Forostyak et. al [13]), containing 40 ng/mL b-FGF (Thermo Fisher PHG0266), 1X B27 supplement (Life Technologies 17504–044) and 10  $\mu$ M retinoic acid (Sigma-Aldrich R2625) in neurobasal medium.

## Secretome collection, enzyme-linked immunosorbent assay (ELISA), and encapsulation efficiency

Secretome was collected from well plates, cell debris was removed using centrifugation (4 mins, 1000 rpm) and samples were placed at  $-20^{\circ}\text{C}$  for short term or  $-80^{\circ}\text{C}$  for long-term storage. Prior to use, secretome was concentrated in centrifugal filters (Fisher Scientific UFC800324) by spinning for 20 minutes at  $4000 \times g$  and  $4^{\circ}\text{C}$ . As a preliminary assessment for potential regenerative growth factor levels were determined via BDNF (Ray Biotech ELH-BDNF-2) and VEGF (Thermo Fisher KHG0111) ELISAs according to manufacturer protocols. VEGF was run at a dilution factor DF=2 for plain neurobasal and DF=5 for modified media samples.

To determine encapsulation efficiency for secretome in PLGA, synthesized particles were dissolved at 50  $\mu\text{g}/\mu\text{L}$  in 1 M NaOH on a shaker for 20 minutes. Samples were neutralized with HCl and diluted with water to a concentration of 10 mg particles/300  $\mu\text{L}$  solution, then

further diluted 1:15 in water for use in a micro-bicinchoninic acid assay (Thermo Fisher 23235), performed per manufacturer's instructions. The same plate was used to determine total protein content for secretome samples (diluted 1:150).

## Statistics

JMP and GraphPad Prism were used for statistical comparisons and graphical representations. ANOVA (for PLGA particle size), Welch's t-test (for ELISA data), or repeated measures ANOVA (for *in vivo* data, iPN groups only) was performed followed by post-hoc Tukey's HSD/t-tests for each group or time point. Statistical significance was considered as  $p\text{-value} < 0.05$ .

## Results

IVIS results indicated that PLGA encapsulation significantly slowed short-term release of dye from hydrogels (Figure 1a/b), as expected. A significant difference between normalized radiant efficiencies of PLGA-encapsulated dye in hydrogel versus non-encapsulated dye in hydrogel appeared by 18 minutes after injection ( $p\text{-value} = 0.04$ , Figure 1b). In longer-term release, PLGA-encapsulated samples in hydrogel had a significantly higher radiant efficiency compared to the non-encapsulated samples at 24 hours ( $p\text{-value} = 0.02$ , Figure 1c). Moreover, delivery of dye in hydrogel maintained a 46–86% higher relative signal compared to free dye in saline 12–72 hours post-injection.

A potential interest for iPN is combination with pro-regenerative molecules secreted by ASCs (secretome). Brightfield images of ASCs following incubation in plain neurobasal medium (NB) versus modified medium (MM) showed clear differences in cellular phenotype (Figure 2a). MM consistently caused ASCs to transition from a static state to an elongated, activated state, in each batch of cells tested. ASCs secreted less than 5 ng/mL BDNF in all incubation cases, with only one batch difference (B1 versus B3, NB,  $p\text{-value} < 0.05$ ) and no differences from MM priming (Figure 2b). However, VEGF secretion was remarkably higher in the MM conditions compared to NB ( $p\text{-value} < 0.0001$  for overall group comparison) with minimal batch-to-batch variation (Figure 2c). To encapsulate temperature-sensitive molecules like secretome, we adapted our PLGA encapsulation protocol to include incubations performed on ice. Imaging of particles confirmed that there was no significant difference in the size of particles produced at room temperature versus on ice (Figure 2d). Particle sizes were  $2.22 \pm 0.72$  and  $2.55 \pm 0.92$   $\mu\text{m}$  for room temperature and ice protocols, respectively, as measured by random particle selection ( $n=30$ /group across three fields). Maximum encapsulation efficiency in PLGA was 28% with the ASC, MM secretome.

## Discussion

Previous experimentation has suggested that iPN hydrogels have about four times shorter biodegradability than that of collagen-I hydrogels, as measured by time needed to reach 50% mass in simultaneous *in vitro* degradation studies [6]. This is advantageous to allow for native ECM deposition after cellular infiltration. Moreover, iPN hydrogels had some mass remaining in solution between 15 and 30 days after gel formation. These *in vitro* degradation

properties are suitable for matrix stabilization and drug delivery in the CNS, given the dynamic tissue remodeling that occur in the CNS as cells begin to invade the lesion space. Future work will be critical to investigate the correlation between the *in vitro* degradation profiles and how the hydrogel behaves in a CNS lesion space (i.e., *in vivo*). In this study, the subcutaneous injection study results provided promising insights for iPN *in vivo* use. Clearly defined boundaries for the hydrogels can be noted in the ROIs provided on the IVIS. Tissue harvest three days post injection also confirmed hydrogel gelation *in vivo* with clear cellular infiltration (Supplemental Figure S1).

Additionally, PLGA encapsulation demonstrated therapeutic payload delivery over the course of multiple days. Many growth factors inherently have short half-lives [14], therefore this longer time range will maximize the influence these factors can have upon delivery to CNS tissue. This study only investigated release of a small molecular weight dextran, meant to mimic growth factors of interest (<50 kDA) because of their similar molecular weights. It is likely that release dynamics will change some for growth factors of various sizes; however, the relative pattern of longer release for PLGA encapsulated molecules versus non-encapsulated molecules is expected to be conserved. Because the dextran-dye is fluorescent – both when encapsulated in PLGA and in its free state – this study does not investigate the degradation of PLGA or release of biomolecules from PLGA, but rather provides data on the release of the dye (combined with PLGA) from iPN hydrogels. Once ASC secretome products or specific growth factors have been identified as desired payloads, it will be necessary to investigate how the presence of PLGA encapsulation influences overall release and bioactivity, given that PLGA will likely biodegrade slower than release of the payload from the iPN hydrogels.

One potential avenue for generating a regenerative cocktail is using secretome. ASCs secrete low, yet potentially effective levels of BDNF in their basal and activated states [15,16], on par with this study. Although incubation with modified medium did not significantly change ASC secretion of BDNF, it did drastically increase VEGF secretion, suggesting that the ASCs were still primed for a regenerative phenotype. While VEGF indirectly influences neural tissue regeneration via vascular repair [17], perhaps other stimulation techniques such as electrical stimulation may be useful in encouraging ASCs to produce factors specific to neural/neurite growth [18]. Additionally, it is possible that modified medium alone (without ASC incubation) may be effective for inciting neural regrowth. Our supplemental data with differentiated SY5Y cells indicated that plain neurobasal medium significantly decreased neurite outgrowth compared to the positive control; however, neurobasal medium incubated on ASCs and modified medium alone were not statistically different from the positive control (Supplemental Figure S2).

Other studies have determined that various growth factors, such as VEGF, BDNF, and GDNF (found in ASC secretome), remain bioactive after PLGA encapsulation [19,20]. This is promising for the potential use of PLGA to encapsulate secretome for combination with iPN. While secretome was successfully encapsulated into PLGA particles by adapting our protocol for temperature-sensitive molecules, the maximum loading efficiency for cell secretome was only 28%. Therefore, other protocol adaptations or pre-designed growth factor cocktails may be necessary to achieve maximal influence via combination therapy.

Additionally, the *in vivo* study results were promising for biomolecule delivery over the course of a few days, but for molecules that need to be delivered over a longer course, PLGA may not be suitable for encapsulation when used with iPN specifically. Next steps will be to investigate ASC secretome or targeted growth factor regimes in combination with iPN for specific CNS injuries. This will determine the synergistic benefits of combining iPN with bioactive substrates and determine the need for PLGA encapsulation as part of individualized therapeutic regimes.”

## Conclusion

The results of this study demonstrated successful injection and subsequent gelation of our iPN hydrogel formulation *in vivo*. PLGA encapsulation may be a promising avenue for combining iPN with pro-regenerative biomolecules or ASC secretome; however, future work must focus on optimal loading conditions and release profiles from the soft hydrogels. Next steps will be applying iPN in various combination therapies for neural tissue repair after spinal cord injury.

## Supplementary Material

Refer to Web version on PubMed Central for supplementary material.

## Acknowledgements

This study was funded by NIH R21 NS111398. We would like to acknowledge Blanca Ostmark for helping with animal handling and protocols and Dr. Keith March (UF Medicine) for discussions and insights into the use of adipose-derived stem cells. We thank Thermo Fisher Aspire program for providing VEGF ELISA materials. The graphical abstract was prepared using BioRender.

## References

- [1]. Peterson AB, Thomas KE, and Zhou H, “Surveillance Report of Traumatic Brain Injury-related Deaths by Age Group, Sex, and Mechanism of Injury -- United States, 2018 and 2019,” Centers for Disease Control and Prevention, 2022.
- [2]. Hlavac N, Kasper M, and Schmidt CE, “Progress toward finding the perfect match: hydrogels for treatment of central nervous system injury,” *Materials Today Advances*, vol. 6, p. 100039, 2020, 10.1016/j.mtadv.2019.100039
- [3]. Kline AE, Leary JB, Radabaugh HL, Cheng JP, and Bondi CO, “Combination therapies for neurobehavioral and cognitive recovery after experimental traumatic brain injury: Is more better?,” *Progress in Neurobiology*, vol. 142, pp. 45–67, 2016, 10.1016/j.pneurobio.2016.05.002 [PubMed: 27166858]
- [4]. Griffin JM and Bradke F, “Therapeutic repair for spinal cord injury: combinatory approaches to address a multifaceted problem,” *EMBO Molecular Medicine*, vol. 12, no. 3, p. e11505, 2020, 10.15252/emmm.201911505 [PubMed: 32090481]
- [5]. McCrary MW, Vaughn NE, Hlavac N, Song YH, Wachs RA, and Schmidt CE, “Novel Sodium Deoxycholate-Based Chemical Decellularization Method for Peripheral Nerve,” *Tissue Engineering Part C: Methods*, vol. 26, no. 1, pp. 23–36, 2019, 10.1089/ten.tec.2019.0135 [PubMed: 31724493]
- [6]. Bousalis D et al. , “Decellularized peripheral nerve as an injectable delivery vehicle for neural applications,” *Journal of Biomedical Materials Research Part A*, vol. 110, no. 3, pp. 595–611, 2022, 10.1002/jbm.a.37312 [PubMed: 34590403]

- [7]. Cerqueira SR et al. , “Decellularized peripheral nerve supports Schwann cell transplants and axon growth following spinal cord injury,” *Biomaterials*, vol. 177, pp. 176–185, 2018, 10.1016/j.biomaterials.2018.05.049 [PubMed: 29929081]
- [8]. Kumar LP, Kandoi S, Misra R, V. S., R. K., and R. S. Verma, “The mesenchymal stem cell secretome: A new paradigm towards cell-free therapeutic mode in regenerative medicine,” *Cytokine & Growth Factor Reviews*, vol. 46, pp. 1–9, 2019, 10.1016/j.cytogfr.2019.04.002 [PubMed: 30954374]
- [9]. Salgado AJBOG, Reis RLG, Sousa NJC, and Gimble JM, “Adipose tissue derived stem cells secretome: soluble factors and their roles in regenerative medicine.,” *Curr Stem Cell Res Ther*, vol. 5, no. 2, pp. 103–110, 2010, 10.2174/157488810791268564 [PubMed: 19941460]
- [10]. Si Z et al. , “Adipose-derived stem cells: Sources, potency, and implications for regenerative therapies,” *Biomedicine & Pharmacotherapy*, vol. 114, p. 108765, 2019, 10.1016/j.biopha.2019.108765 [PubMed: 30921703]
- [11]. di Summa PG, Kalbermatten DF, Raffoul W, Terenghi G, and Kingham PJ, “Extracellular Matrix Molecules Enhance the Neurotrophic Effect of Schwann Cell-Like Differentiated Adipose-Derived Stem Cells and Increase Cell Survival Under Stress Conditions,” *Tissue Engineering Part A*, vol. 19, no. 3–4, pp. 368–379, 2012, 10.1089/ten.tea.2012.0124 [PubMed: 22897220]
- [12]. Kingham PJ, Kolar MK, Novikova LN, Novikov LN, and Wiberg M, “Stimulating the Neurotrophic and Angiogenic Properties of Human Adipose-Derived Stem Cells Enhances Nerve Repair,” *Stem Cells and Development*, vol. 23, no. 7, pp. 741–754, 2013, 10.1089/scd.2013.0396 [PubMed: 24124760]
- [13]. Forostyak O et al. , “Specific profiles of ion channels and ionotropic receptors define adipose- and bone marrow derived stromal cells,” *Stem Cell Research*, vol. 16, no. 3, pp. 622–634, 2016, 10.1016/j.scr.2016.03.010 [PubMed: 27062357]
- [14]. Ren X, Zhao M, Lash B, Martino MM, and Julier Z, “Growth Factor Engineering Strategies for Regenerative Medicine Applications,” *Frontiers in Bioengineering and Biotechnology*, vol. 7, 2020, [Online]. Available: 10.3389/fbioe.2019.00469
- [15]. Lopatina T et al. , “Adipose-Derived Stem Cells Stimulate Regeneration of Peripheral Nerves: BDNF Secreted by These Cells Promotes Nerve Healing and Axon Growth De Novo,” *PLOS ONE*, vol. 6, no. 3, pp. e17899-, Mar. 2011, [Online]. Available: 10.1371/journal.pone.0017899 [PubMed: 21423756]
- [16]. Wei X et al. , “IFATS Collection: The Conditioned Media of Adipose Stromal Cells Protect Against Hypoxia-Ischemia-Induced Brain Damage in Neonatal Rats,” *Stem Cells*, vol. 27, no. 2, pp. 478–488, Feb. 2009, doi: 10.1634/stemcells.2008-0333. [PubMed: 19023032]
- [17]. Salehi A, Zhang JH, and Obenaus A, “Response of the cerebral vasculature following traumatic brain injury,” *Journal of Cerebral Blood Flow & Metabolism*, vol. 37, no. 7, pp. 2320–2339, Apr. 2017, doi: 10.1177/0271678X17701460. [PubMed: 28378621]
- [18]. Hlavac N et al. , “Effects of Varied Stimulation Parameters on Adipose-Derived Stem Cell Response to Low-Level Electrical Fields,” *Annals of Biomedical Engineering*, vol. 49, no. 12, pp. 3401–3411, Dec. 2021, doi: 10.1007/s10439-021-02875-z. [PubMed: 34704163]
- [19]. Arranz-Romera A et al. , “A Safe GDNF and GDNF/BDNF Controlled Delivery System Improves Migration in Human Retinal Pigment Epithelial Cells and Survival in Retinal Ganglion Cells: Potential Usefulness in Degenerative Retinal Pathologies,” *Pharmaceuticals (Basel)*, vol. 14, no. 1, p. 50, Jan. 2021, doi: 10.3390/ph14010050. [PubMed: 33440745]
- [20]. Rui J et al. , “Controlled release of vascular endothelial growth factor using poly-lactic-co-glycolic acid microspheres: in vitro characterization and application in polycaprolactone fumarate nerve conduits,” *Acta Biomaterialia*, vol. 8, no. 2, pp. 511–8, Feb. 2012, doi: 10.1016/j.actbio.2011.10.001. [PubMed: 22019759]



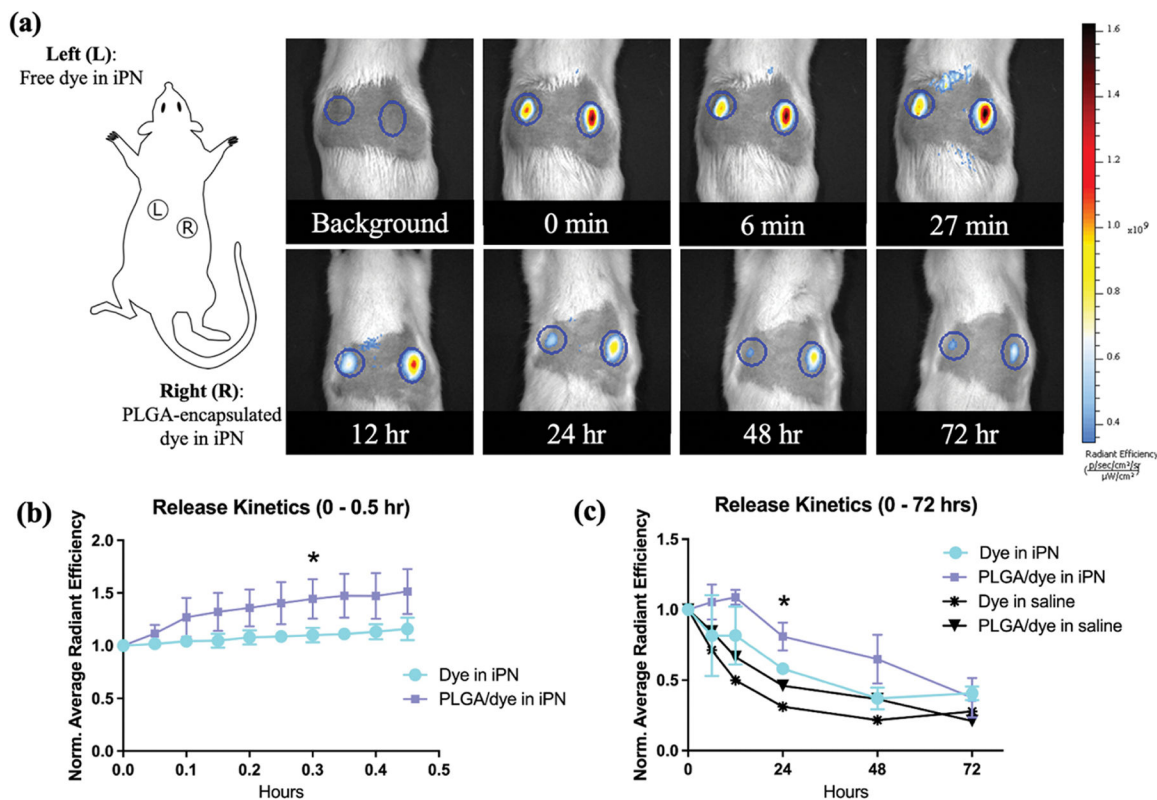


**Figure 1.**

*In vivo* iPN hydrogel injection with and without PLGA-encapsulated dye. **(a)** Adult rats were injected subcutaneously with two 150  $\mu\text{L}$  iPN hydrogel or saline solutions containing free dye or PLGA-encapsulated dye. Example ROIs are shown in the circles and represent the area measured for radiant efficiency (correlated to amount of signal). **(b)** Short-term release profile: images were captured  $10 \times 3$  minutes (0–27 minutes). There was a statistically significant difference in signal beginning at 18 minutes post-injection. **(c)** Long-term release profile: images were obtained over the course of 72 hours. Statistical differences appeared at 24 hours post-injection between the iPN groups, \* $p$ -value<0.05 for iPN with PLGA-encapsulated dye versus iPN with free dye.

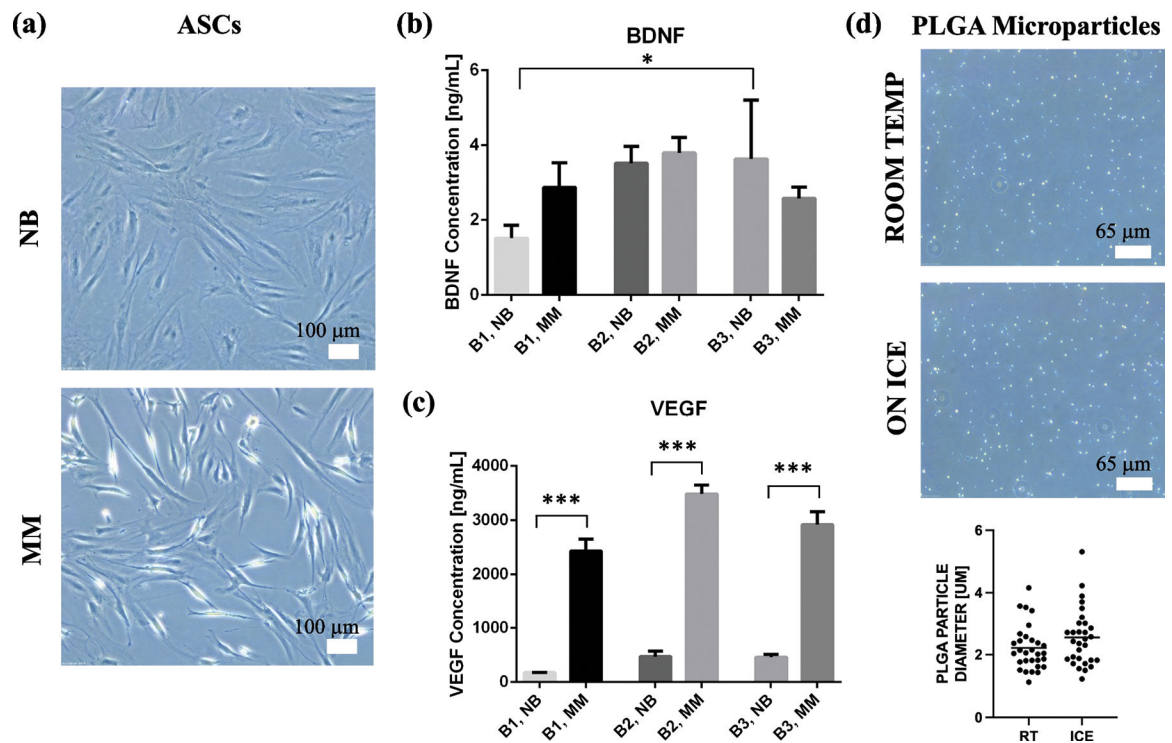


**Figure 2.**

ASC secretome as a potential combination therapy with iPN for neural applications. **(a)** ASC culture in modified medium (MM) with B27, b-FGF and retinoic acid caused a reproducible phenotypic shift from static (cuboidal) to activated (elongated) bodies. **(b)** ELISA results indicated little difference in BDNF secretion between batches (B1, B2, B3) or NB versus MM media. One significant difference, between B1 and B3, arose but with little change in BDNF production, \*p-value<0.05. **(c)** VEGF ELISA results showed marked increase in the ASC group exposed to MM as compared to NB, \*\*\*p-value was <0.0001 for overall group ANOVA. **(d)** The PLGA encapsulation protocol was adapted to include all incubations on ice for biomolecules that may be temperature sensitive. Images of each protocol are shown and average particle size (n=30) for both are graphed.